ELSEVIER

Journal of Power Sources 62 (1996) 161–166

JOURNAL OF POWER SOURCES

Resistance changes and premature capacity loss in lead battery plates

M. Calábek [a], K. Micka [b], P. Bača [a], P. Křivák [a], V. Šmarda [a]

[a] *Technical University of Brno, 662 09 Brno, Czech Republic*

[b] *J. Heyrovský Institute of Physical Chemistry, Academy of Sciences of the Czech Republic, 182 23 Prague 8, Czech Republic*

Received 22 December 1995; revised 10 May 1996; accepted 22 May 1996

Abstract

Our research work has been devoted to the identification of processes that cause premature capacity loss (PCL) in lead/acid batteries. Attention has been paid to the resistance of the active material and to the resistance of the interphase between the active material and the lead grid in specially prepared positive test electrodes, measured by an exact d.c. method. Resistance measurements performed on electrodes with grids from seven different lead alloys showed that PCL is related to increasing resistance of the active material. In contrast, PCL in electrodes having pure-lead grids is caused by the formation of an insulating layer on the grid surface, evidenced by the steeply rising interphase resistance.

Keywords: Lead/acid batteries; Active mass resistance; Interphase resistance; Capacity loss

1. Introduction

Research on lead/acid batteries for electric vehicles is directed towards two main objectives: (i) to increase the specific energy, and (ii) to suppress or to eliminate the effect of premature capacity loss (PCL), which is particularly notable with low-antimony or non-antimonial grid alloys [1,2], used to lower the self discharge. PCL effect can have, in principle, two main causes, namely the formation of barrier layers at the grid-active mass interface (PCL-1), and increase in the resistivity of the active mass (PCL-2). Both the contact resistance, i.e. the resistance of the corrosion layer, and the active mass resistance within the plate can be analysed by a sensitive method that has been developed in the authors' laboratories and verified in many tests on a range of grid alloys [3–6]. Of particular interest are the recent results which revealed the effect of tin on the contact resistance [6]. An attempt to elucidate the causes of PCL effect forms the subject of the present work.

2. Method of measurement

The method of measurement uses pasted laboratory electrodes with specially prepared lead grids, shown schematically in Fig. 1. The grid consists of a parallel arrangement of ribs, held in position by epoxy castings, on to which a typical positive paste is applied. The ribs are numbered 1 to 10 and

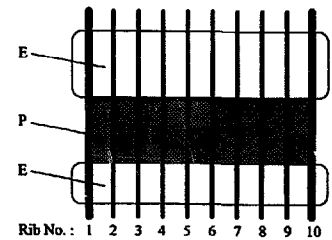

Fig. 1. Schematic diagram of pasted test plate for measurement of resistances. Dimensions of paste area: 55 mm × 20 mm × 7 mm; distance between neighbouring ribs: 5.5 mm. (E) epoxy frame, and (P) porous active material.

resistance is determined through systematic variation of current flow between selected ribs. The older (extrapolation) method [3,6] has been replaced by the new difference method, which is insensitive against any inhomogeneities or cracks in the active mass. The interphase resistance, R_k, is measured on a single rib, and the active material resistance, R_m, is measured between neighbouring ribs, 20 mm long and lying 5.5 mm apart. Since the surface area of each rib is about 96 mm^2, values of R_k roughly correspond to surface resistivity in Ω cm^2. In view of the electrode geometry, the resistivity of the active material in Ω cm may be obtained by multiplying the values of R_m by the factor of 2.5.

Any single resistance measurement consists of three steps:

PII S0378-7753(96)02432-9

(i) Step 1: the measuring current is fed in via rib n ($n=2$–8) and out via rib $n+2$. A voltage, U_1, is measured between ribs n and $n+1$.

(ii) Step 2: the same measuring current is fed in via rib $n-1$ and out via rib $n+2$. A voltage, U_2, is measured between ribs n and $n+1$.

(iii) Step 3: again with the same current, a voltage, U_3, across a calibration resistance, R_C, is measured.

The contact resistance, R_k, of rib n is then calculated according to the formula

$$R_k=\frac{U_1-U_2}{U_3}R_C-R_P \quad (1)$$

where R_P is a correction term due to the resistance of the given rib. An approximate determination of its value was described in detail in Ref. [4]. The resistance, R_m, of the active material between ribs n and $n+1$ is calculated as

$$R_m=\frac{U_2}{U_3}R_C \quad (2)$$

The measurement series can be repeated in the direction of decreasing rib numbers. Thus, in step 1, the current flows between ribs n and $n-2$ ($n=3$–9), and in steps 2 and 3 it flows between ribs $n+1$ and $n-2$. Voltages U_1 and U_2 are measured between ribs n and $n-1$. In this way, ribs 3–8 are subjected to both directions of current flow. Altogether, 42 measuring steps are required for one plate. The deviations between values measured in the two directions are very small, we found $\pm 0.12\%$ for R_k and $\pm 1.1\%$ for R_m on the average for a particular test plate. The difference method allows a high degree of automation based on the use of a personal computer and a computer-controlled current source and relays.

3. Experimental

Test electrodes were pasted on grids from pure lead and seven different grid alloys (Table 1). The area for pasting was 55 mm × 20 mm × 7 mm. The paste had a typical industrial formulation (from Bären Batterie, Austria). The test cells contained a large excess of both electrolyte and negative active material. The negative electrodes were placed at either side of the test electrode at a distance of about 25 mm. No separators were used. The plates were formed in the usual way.

The test electrodes were arranged into two groups (eight electrodes each); one group was cycled under a 'bad' regime and the other under a 'good' one [7]. These were distinguished by the rate of charging. In the bad regime, the charging current was adjusted so that the charge passed after 18 h was equal to 150% of that obtained after discharge in the preceding cycle. In the good regime, the electrodes were charged more rapidly with a current of 0.5 A until the cell voltage reached 2.4 V, and then with a current of 0.25 A so that the total charge was 125% of that obtained during discharge. The electrodes were discharged daily at 1.25 A (about 1 h discharge rate) to a cutoff voltage of 1.6 V (100% depth-of-discharge). The test cells were kept at 35 °C.

The values of R_k and R_m were measured either before the beginning of discharge (at least 3 h after the end of charging) or immediately after its end. Mean values of R_K for eight measured ribs of one plate and mean values of R_m for the seven sections between them were calculated. Regularity in the time schedule of measurements was observed to eliminate slow changes of the resistance with the time [8]. Since the increase in resistance towards the end of the cycle life was often very large, it was considered more suitable to plot the values of conductance, rather than resistance ($G_k=1/R_k$, $G_m=1/R_m$).

4. Results and discussion

Figs. 2–4 show the dependences of the mean interphase conductances of the particular ribs, G_k, and of the mean active mass conductances, G_m, between neighbouring ribs, together with the discharge capacity, C, on the number of cycles for electrodes cycled under the bad regime. The horizontal lines indicate two-thirds of the capacity attained in the seventh cycle; this was considered as the limit of the cycle life. The conspicuous decrease in capacity is here obviously a manifestation of the PCL effect, caused by the bad cycling regime. The vertical lines in Fig. 2 indicate the cycle number after which the bad regime was replaced by a good one. This, as can be seen, did not lead to restoration of the discharge capacity, which is in disagreement with the findings of Winsel et al. [7], who used commercial positive plates of usual thickness, which showed a more rapid fall of capacity during cycling under the bad regime.

With the Pb–Ca and Pb–Ca–Sn–1 grids, a remarkable transient increase in G_k values can be observed between the 52nd and 53rd cycles, corresponding to a nine-day interruption of cycling. With the antimonial grids under the same conditions, there is a corresponding decrease in G_m and G_k values. We observed similar phenomena, in the course of hundreds of

Table 1
Composition (in wt.%) of the lead grid alloys

Grid type	Pure Pb	Pb–Ca	Pb–Ca–Sn–1	Pb–Ca–Sn–2	Pb–Sb–1	Pb–Sb–2	Pb–Sb–3	Pb–Sb–4
Ca		0.09	0.09	0.09				
Sb					1.61	1.68	2.19	5.73
Sn			0.32	0.70	0.37	0.05	0.20	0.27

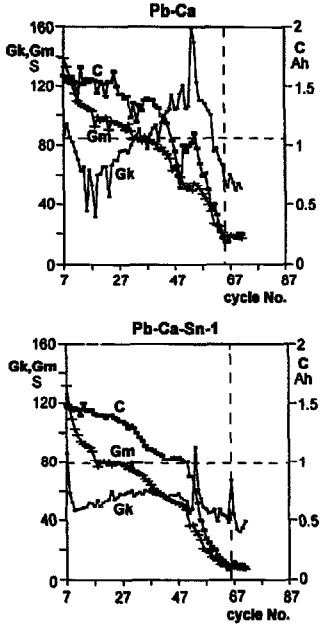

Fig. 2. G_k, G_m and C vs. cycle num' for electrodes with Pb–Ca and Pb–Ca–Sn–1 grids cycled under the oad regime.

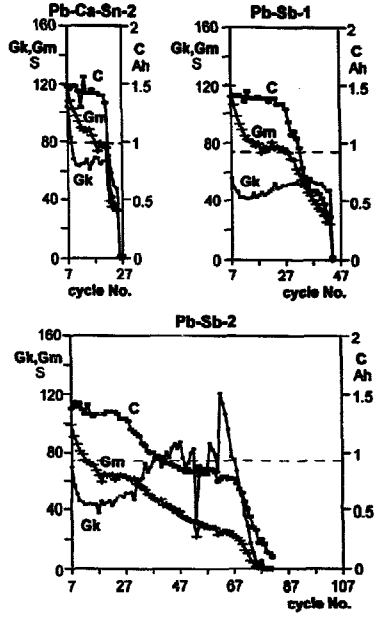

Fig. 3. G_k, G_m and C vs. cycle number for electrodes with Pb–Ca–Sn–2, Pb–Sb–1, and Pb–Sb–2 grids cycled under the bad regime.

hours, already earlier, see Refs. [5,8,9]; the decrease in G_m during a prolonged stand was discussed in detail and attributed to the formation of a thin layer of $PbSO_4$ on the surface of PbO_2 particles [8]. Slow corrosion of the Pb–Sb grid may cause an increase in interphase resistance with time. However, the peculiar behaviour of the Pb–Ca grid interphase resistance is difficult to explain. The time effect is, in general, not well reproducible and it seems to be the result of two counter-acting factors, one of which is a slow corrosion of the lead grid and the other is the physico-chemical state of the lead grid surface and of the interphase involving adsorbed substances or impurities which may influence both the corrosion rate and the conductivity of the corrosion products.

A close resemblance between the curves of the capacity and of the active material conductance can be observed. The correlation between the values of G_m and the normalized discharge capacity, C/C_0 (where C_0 denotes the 'initial' capacity measured in the seventh cycle), is illustrated in Fig. 5: the capacity increases linearly with the conductance of the (charged) active material up to the value of $G_m \approx 80$ S and then it remains almost constant. This is particularly true for electrodes with Pb–Ca, Pb–Ca–Sn–1, Pb–Ca–Sn–2, and Pb–Sb–1 grids. Takahashi et al. [10] published a plot of discharge time against positive active material resistance (without specifying the method of measurement) showing essentially the same phenomenon. A similar finding was reported later by Winsel et al. [7], who used the d.c. potential probe method, but they did not clearly distinguish between the resistance of the active material and that of the interphase layer. The increase in resistance of the active material with cycle number is doubtless related with the decrease in apparent density reported already by Dittmann and Sams [11], which is manifested by increasing plate thickness [12,13]. This leads to deterioration of interparticle contacts and, eventually, to degradation of the porous electrode structure.

Similar dependences were obtained for electrodes cycled under the good regime, but their cycle life was appreciably longer, except for the electrode with Pb–Ca grid, which surprisingly broke down after several cycles. This suggests that rapid charging in this case is not sufficient to remove the lead sulfate layer at the grid surface. With respect to 100% depth-of-discharge, the other electrodes attained a rather high cycle life, as can be seen from Fig. 6 (for Pb–Ca–Sn–1 and 2 grids) and Fig. 7 (for Pb–Sb–1 and 4 grids, which behaved as Pb–Sb–2 and 3). Shedding of the active material, but no deterioration of the current collector, was observed at the end of the test.

A summary of cycle lives of the electrodes under study cycled under either regime is shown graphically in Fig. 8; it

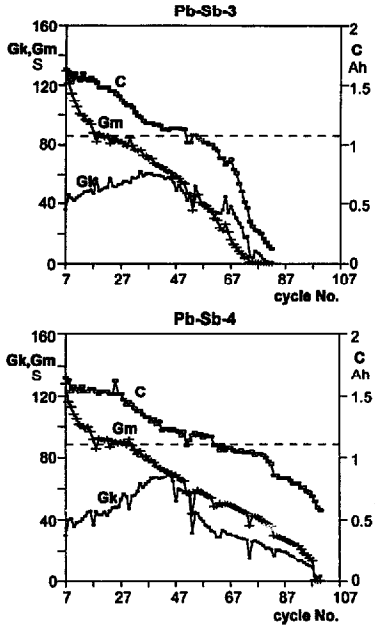

Fig. 4. G_k, G_m and C vs. cycle number for electrodes with Pb–Sb–3 and Pb–Sb–4 grids cycled under the bad regime.

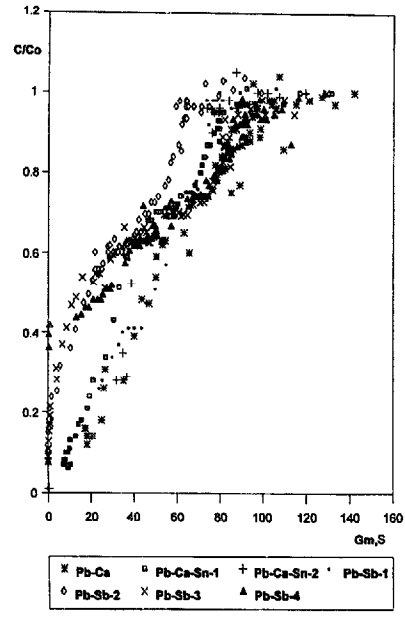

Fig. 5. Normalized capacity vs. active mass conductance for electrodes cycled under the bad regime.

can be seen that for antimonial lead collectors under the bad regime, the cycle life increases with antimony content as could be expected [14]. The beneficial effect of tin, on the other hand, is only manifested under the good regime.

Electrodes with pure-lead grids broke down before finishing the six conditioning cycles. Their capacity fell in parallel with the conductances. G_k and G_m. These results strongly suggest the presence of some form of passivation of the lead grid. Further evidence of passivation was obtained from voltage–time curves which were of the usual shape, but shifted to lower voltage values (Fig. 9). Such behaviour is typical for passivation due to the formation of high-resistance layers close to the grid [15,16]. A similar observation was made by Dimitrov and Pavlov [17], who concluded, therefore, that PCL is caused by phenomena in the corrosion layer in general, but we cannot share this opinion; our experiments suggest that the case of the pure-lead grid is an exceptional one. Anodic corrosion layers on pure-lead electrodes in sulfuric acid were often studied; under a primarily formed $PbSO_4$ layer, a layer of tetragonal PbO or mPbO · nPbSO$_4$ is formed after depletion of sulfuric acid caused by transport hindrance. This layer is responsible for ohmic polarization or passivation of the lead electrode [18–21]; a layer of PbO_2 instead of $PbSO_4$ is formed at higher anodic potentials [6,21].

With electrodes containing alloyed lead grids, a fall in the discharge capacity was accompanied by a decrease in conductance of the active material, whereas no correlation with the interphase conductance was found. Under the bad regime, the G_k values usually began to fall only when the end of the cycle life, i.e. 2/3 of C_0, was attained. Under the good regime, the changes of G_k values were relatively small or, with antimonial lead grids, even negligible. The relatively high values of G_k are doubtless related with both the beneficial effect of antimony, which suppresses the formation of the PbO layer [6], and the beneficial effect of tin, which improves its conductivity [16,22,23]. At the end of the cycle life, the contacts between most of the active material particles were apparently disrupted, since shedding of the active material was observed. This caused the drop of G_m values.

The decrease in capacity under the bad cycling regime is a typical manifestation of the PCL effect, although, as anticipated, the rate of capacity loss was lower for antimonial lead grids. The clear correlation with the active material conductance (Fig. 5) is in line with active material-based causes of capacity loss (PCL-2), discussed extensively by the German authors using a sophisticated model that takes into account the quality of contacts between active material particles and their dependence on the polarizing current and

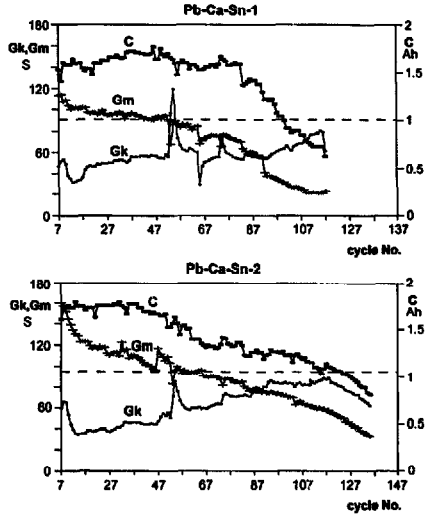

Fig. 6. G_k, G_m and C vs. cycle number for electrodes with Pb–Ca–Sn–1 and Pb–Ca–Sn–2 grids cycled under the good regime.

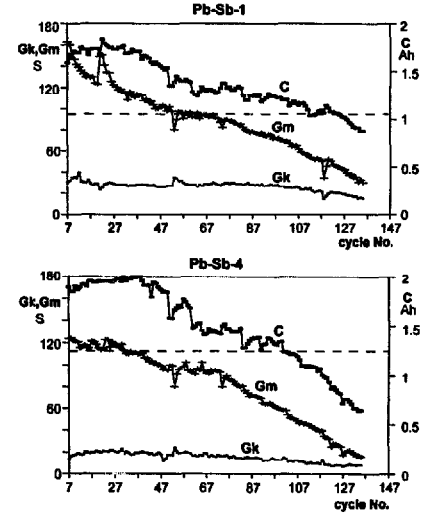

Fig. 7. G_k, G_m, and C vs. cycle number for electrodes with Pb–Sb–1 and Pb–Sb–4 grids cycled under the good regime.

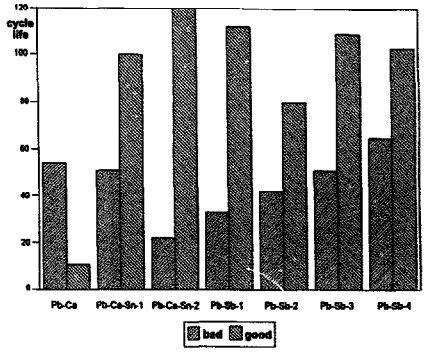

Fig. 8. Cycle life of electrodes with various grid alloys cycled under the bad and good regimes.

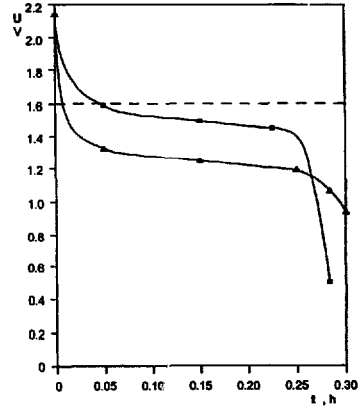

Fig. 9. Discharge curves for two electrodes with pure-lead grids.

potential [7,24,25]. (Experiments carried out under the good cycling regime lead to a similar conclusion.)

A theory of the effect of active material resistance on the discharge capacity, based on an electrical equivalent circuit representing the porous electrode, was elaborated already earlier by Bouet and Pompon [26], who took into account the resistance increase during discharge and during cycling, the structural changes during cycling, and the mass and charge transport. The authors concluded that the loss of capacity is largely due to an increase in the resistance of intergranular contacts and not to a decrease in the electrochemical activity of lead dioxide, assumed by some earlier authors [27,28]. This is in agreement with the above statements.

A study of the influence of the discharge rate on the resistance measurements and of the scatter of the R_k values for individual ribs will be the subject of our next communication.

5. Conclusions

Our experiments substantiated the findings of earlier authors that the so-called bad cycling regime, characterized by a low charging rate, leads to premature capacity loss of positive lead/acid battery electrodes.

Conductance measurements on laboratory positive plates with grids from seven different lead alloys, performed by an exact method, showed that the loss of capacity, under either bad or good cycling regime, is strongly associated with decreasing conductance of the active material. The interphase conductance either does not change appreciably during cycling or begins to drop only at the end of the cycle life.

The results make the 'barrier layer model' (PCL-1) much less probable than the 'active mass resistivity model' (PCL-2) [1,2] for elucidation of PCL.

With electrodes containing pure-lead grids, a rapid loss of capacity was observed, apparently caused by grid passivation, as evidenced by the extremely high interphase resistance as well as by the discharge potential–time curves.

6. List of symbols

C	discharge capacity, Ah
C_0	discharge capacity at the seventh cycle, Ah
G_k	conductance of interphase layer on one rib, Ω^{-1}
G_m	conductance of active material between two ribs, Ω^{-1}
n	rib number
R_C	calibration resistance
R_k	resistance of interphase layer on one rib, Ω
R_m	resistance of active material between two ribs, Ω
R_P	rib resistance, Ω
$U_{1,2}$	voltage drops between two neighbouring ribs under different conditions, V
U_3	voltage drop across calibration resistance, V

Acknowledgements

This work was supported by the Advanced Lead–Acid Battery Consortium (in Project No. AMC-003A), a program of the International Lead Zinc Research Organization, and by the Grant Agency of the Czech Republic.

References

[1] A.F. Hollenkamp, *J. Power Sources, 36* (1991) 567.
[2] A.F. Hollenkamp, K.K. Constanti, A.M. Huey, M.J. Koop and L. Apateanu, *J. Power Sources, 40* (1992) 125.
[3] K. Micka and M. Calábek, *J. Power Sources, 30* (1990) 315.
[4] M. Calábek and K. Micka, *Electrochim. Acta, 37* (1992) 1805.
[5] M. Calábek and K. Micka, *Proc. Int. Conf. Lead/Acid Batteries: LABAT '93, St. Konstantin, Varna, Bulgaria, 7–11 June 1993*, pp. 38–41.
[6] A.F. Hollenkamp, K.K. Constanti, M.J. Koop, L. Apateanu, M. Calábek and K. Micka, *J. Power Sources, 48* (1994) 195.
[7] A. Winsel, E. Voss and U. Hullmeine, *J. Power Sources, 30* (1990) 209.
[8] M. Calábek and K. Micka, *J. Power Sources, 30* (1990) 309.
[9] M. Calábek, K. Micka, P. Bača and V. Šmarda, *ALABC Project AMC-003A, Final Rep., 1 July 1994–30 June 1995*, Technical University of Brno, Czech Republic, Aug. 1995.
[10] K. Takahashi, M. Tsubota, K. Yonezu and K. Ando, *J. Electrochem. Soc., 130* (1983) 2144.
[11] J.F. Dittmann and J.F. Sams, *J. Electrochem. Soc., 105* (1958) 553.
[12] K. Micka, M. Svatá and V. Koudelka, *J. Power Sources, 4* (1979) 43.
[13] D. Pavlov and E. Bashtavelova, *J. Electrochem. Soc., 133* (1986) 241.
[14] S.R. Ellis, N.A. Hampson, M.C. Ball and F. Wilkinson, *J. Appl. Electrochem., 16* (1986) 159.
[15] J. Garche, N. Anastasijević and K. Wiesener, *Electrochim. Acta, 26* (1981) 1363.
[16] H. Döring, J. Garche, H. Dietz and K. Wiesener, *J. Power Sources, 30* (1990) 41.
[17] M.K. Dimitrov and D. Pavlov, *J. Power Sources, 46* (1993) 203.
[18] P. Ruetschi and R.T. Angstadt, *J. Electrochem. Soc., 111* (1964) 1323.
[19] D. Pavlov, *Electrochim. Acta, 13* (1968) 2051.
[20] D. Pavlov and R. Popova, *Electrochim. Acta, 15* (1970) 1483.
[21] R.L. Deutscher, S. Fletcher and J.A. Hamilton, *Electrochim. Acta, 31* (1986) 585.
[22] R.T. Barton, P.J. Mitchell and F.A. Fleming, *Power Sources, 13* (1991) 25; *Chem. Abstr., 118* (1993) 208 Abstr. No. 10.
[23] P. Simon, N. Bui and F. Dabosi, *J. Power Sources, 50* (1994) 141.
[24] E. Meissner and E. Voss, *J. Power Sources, 33* (1991) 231.
[25] E. Meissner and H. Rabenstein, *J. Power Sources, 40* (1992) 157.
[26] J. Bouet and J.P. Pompon, *Electrochim. Acta, 26* (1981) 1477.
[27] S.M. Caulder and A. C. Simon, *J. Electrochem. Soc., 121* (1974) 1546.
[28] J. Yamashita, H. Yufu and T. Matsumaru, *J. Power Sources, 30* (1990) 13.